Support Information

The catalytic evaluation of bimetallic Pd-based nanocatalysts supported on ion exchange resin in nitro and alkyne reduction reactions

Tábata R. Silva, Daniela C. de Oliveira, Tarasankar Pal and Josiel B. Domingos

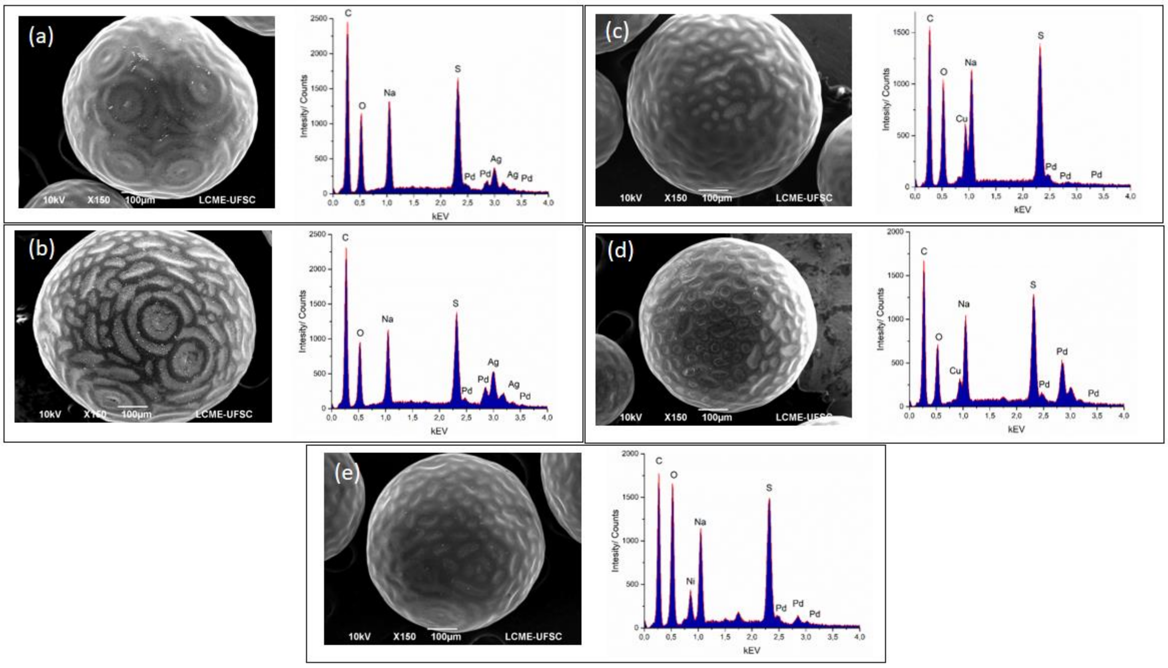

Figure S1. SEM micrographs and their respective EDS spectra of synthesized bimetallic nanocatalysts: (a) AgPd@R, (b) PdAg@R, (c) CuPd@R, (d) PdCu@R and (e) NiPd@R.

Table S1. Content of metal species in the catalysts determined by FAAS.

Catalysts		%(m/m)			
		Ag	Cu	Ni	Pd
Monometallic	Ag@R	0.23	--	--	--
	Cu@R	--	0.07	--	--
	Ni@R	--	--	0.06	--
	Pd@R	--	--	--	0.08
Bimetallic	AgPd@R	0.11	--	--	0.05
	PdAg@R	0.07	--	--	0.09
	CuPd@R	--	0.084	--	0.06
	PdCu@R		0.10		0.06
	NiPd@R	--	--	0.08	0.10
	PdNi@R	--	--	0.05	0.06

Table S2. Percentage ratio of the metals on the surface of the catalysts (%m/m) determined by XPS and their respective binding energies (eV).

	Elements								
	$Ag_{3d\ 5/2}$		$Cu_{2p\ 3/2}$			$Ni_{2p\ 3/2}$		$Pd_{3d\ 5/2}$	
Sample	Ag/Pd	B.E	Cu/Pd	Cu^{+}/Cu^{+2}	B.E	Ni/Pd	B.E	Pd^{0}/Pd^{+2}	B.E
Ag@R	--	368.3 Ag^{+}	--	--	--	--	--	--	--
AgPd@R	8.6	367.8 Ag^{+}	--	--	--	--	--	1	335.0 Pd^{0}
PdAg@R	2	368 Ag^{+}	--	--	--	--	--	1	335.6 Pd^{0}
Cu@R	--	--	--	1.2	932.8 Cu^{+} 934.6 Cu^{2+}	--	--	--	--
CuPd@R	--	--	1.1	0.33	932.2 Cu^{+} 934.1 Cu^{2+}	--	--	1	335.6 Pd^{0}
PdCu@R	--	--	1.2	3.2	932.7 Cu^{+} 934.4 Cu^{2+}	--	--	1	335.5 Pd^{0}
Ni@R	--	--	--	--	--	--	856.3 Ni^{+2}	--	--
NiPd@R	--	--	--	--	--	14.6	856.6 Ni^{+2}	0.64	335.1 Pd^{0} 337.2 Pd^{2+}
Pd-Ni@R	--	--	--	--	--	10.1	856.6 Ni^{+2}	--	336.1 $Pd^{\delta+}$
Pd@R	--	--	--	--	--	--	--	3.7	334.8 Pd^{0} 336.8 Pd^{2+}

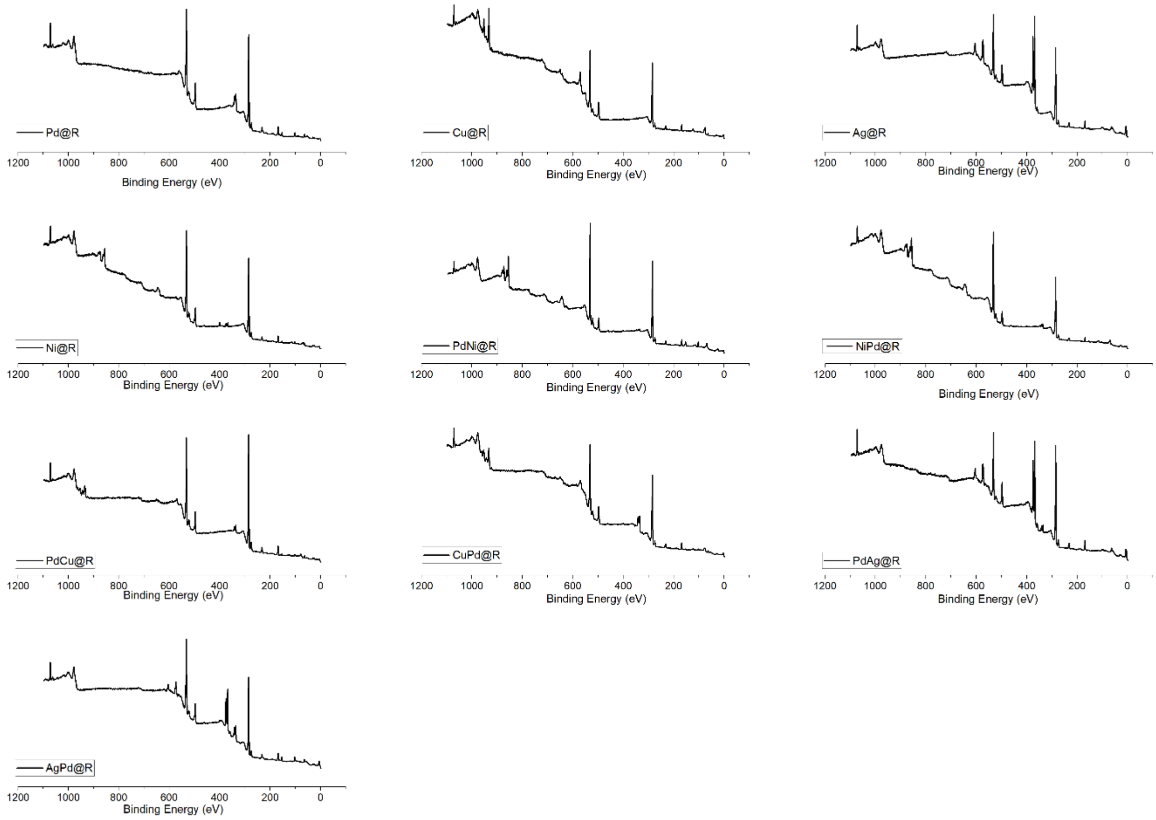

Figure S2. XPS survey spectra for all catalysts.

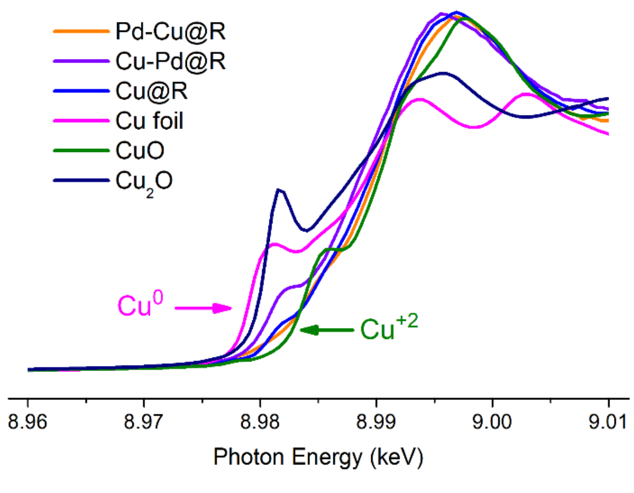

Figure S3. XANES spectra at Cu-edge for the Cu-based catalysts, Cu foil and CuO and Cu_2O standards.

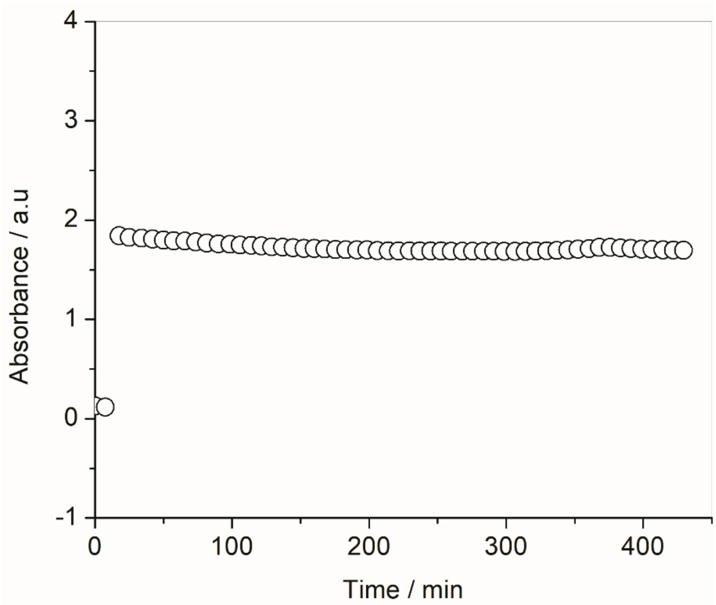

Figure S4. Variation in absorbance at 400 nm as a function of time in minutes with addition of ([Nip] = 0.1 mmol L-^{1}, [$NaBH_4$] = 100 mmol L^{-1}, [Resin] = 2 x 10^{-3} mg L $^{-1}$) in the absence of Pd NPs in water at 15 ° C].

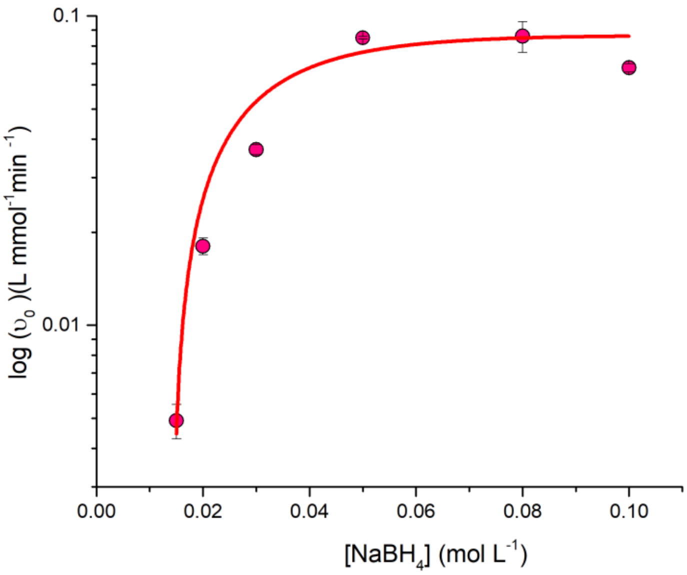

Figure S5. k_{app} for the reduction of Nip as a function of [$NaBH_4$] ([Nip] = 0.1 mmol L^{-1}, [Cu@R] = 1.53 mg L^{-1}, at 15 °C, in water).

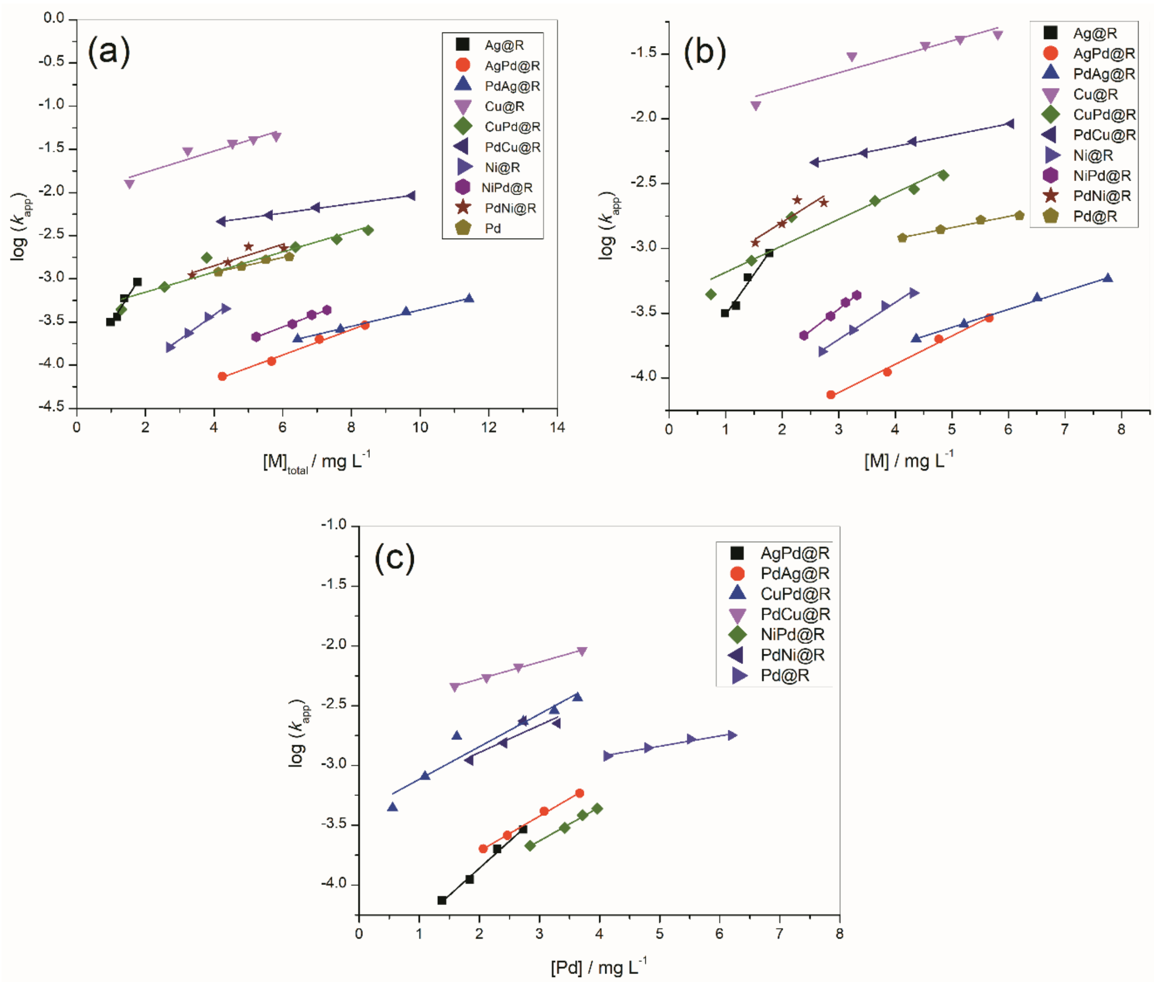

Figure S6. k_{app} for the Nip catalytic reduction reaction as a function of: (a) the total concentration of metals; (b) selected metals (Ag, Cu, Ni) and (c) the concentration of Pd. ([Nip] = 0.1 mmol L^{-1}, [$NaBH_4$] = 100 mmol L^{-1}, at 15 ºC).

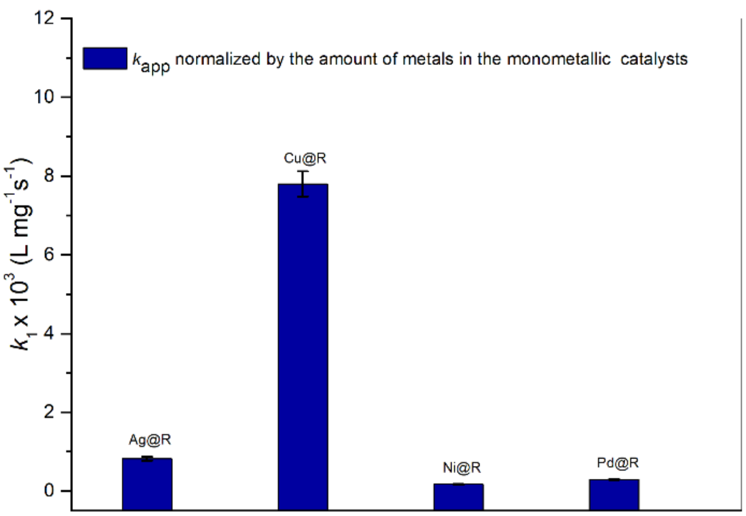

Figure S7. Catalytic activity (k_1) of resin-supported nanoparticles considering the total amount of metals for the monometallic nanoparticles for the Nip reduction reaction.

Table S3. Catalytic activity (TOF / min^{-1}) for mono and bimetallic resin supported nanoparticles in the styrene hydrogenation considering the total amount of metals (Total), only the amount of Ag, Cu, Ni (M) or the amount of Pd.

Entry	Catalyst	TOF_{total}[a]	TOF_{M}[b]	TOF_{Pd}[c]
1	Pd@R	0.55	0.55	--
2	Ag@R	0	--	--
3	Ni@R	0	--	--
4	Cu@R	0	--	--
5	AgPd@R	0.002	0.0047	0.0099
6	PdAg@R	0	--	--
7	NiPd@R	0.60	0.093	1.47
8	PdNi@R	0.53	0.67	1.84
9	CuPd@R	0.017	0.045	0.07
10	PdCu@R	0	0	0

[a]TOF_{total}, moles of product converted per moles of metals and time. [b]TOF_{M}, moles of product converted per moles of Ag, Ni or Cu and time. [c]TOF_{Pd}, moles of product converted per moles of Pd and time.

Table S4. Summary of results reported for semihydrogenation of phenylacetylene with heterogeneous bimetallic palladium-based catalysts.

Entry	Catalyst	TOF[a] (min^{-1})	Selectivity to styrene (%)	Reference
1	Pd@R	9.23	0	This work
2	NiPd@R	4.55	7	This work
3	PdNi@R	16.95	0	This work
4	CuPd@R	0.14	91	This work
5	PdCu@R	0.57	93	This work
6	$Fe_3O_4@SiO_{2(c,80)}PdCu_6$	90	90	1
7	$Fe_3O_4@SiO_{2(c,80)}PdCu_{0.6}$	223.8	82	1
8	$PdCu_4/SiO_2$	0.83	97	2
9	$PdCu_6/Al_2O_3$	120	90	3
10	$PdCu_2/Al_2O_3$	48	90	4
11	Cu-PdNPs@MCM-48	0.077	90	5
12	Cu-PdNPs@MagSilica	0.045	98	5
13	$Pd_{2.7}Ni/N/C$	1.1	87	6
14	Lindlar catalyst	12.7	56	7

[a]The amount of metal is based on the moles of metal components involved.

References

1 L. Yang, X. Chen, Z. Zhou, R. Zhang, L. Li, Z. Cheng and X. Fang, *ChemistrySelect*, 2016, **1**, 5599-5606.
2 F. P. da Silva, J. L. Fiorio, R. V. Gonçalves, E. Teixeira-Neto and L. M. Rossi, *Industrial & Engineering Chemistry Research*, 2018, **57**, 16209-16216.
3 Z. Wang, L. Yang, R. Zhang, L. Li, Z. Cheng and Z. Zhou, *Catalysis Today*, 2016, **264**, 37-43.
4 P. V. Markov, G. O. Bragina, A. V. Rassolov, G. N. Baeva, I. S. Mashkovsky, V. Y. Murzin, Y. V. Zubavichus and A. Y. Stakheev, *Mendeleev Communications*, 2016, **26**, 502-504.
5 E. Buxaderas, M. A. Volpe and G. Radivoy, *Synthesis*, 2019, **51**, 1466-1472.
6 W. Wu, W. Zhang, Y. Long, J. Qin, H. Wen and J. Ma, *Journal of Colloid and Interface Science*, 2018, **531**, 642-653.
7 Q. Feng, S. Zhao, Y. Wang, J. Dong, W. Chen, D. He, D. Wang, J. Yang, Y. Zhu, H. Zhu, L. Gu, Z. Li, Y. Liu, R. Yu, J. Li and Y. Li, *Journal of the American Chemical Society*, 2017, **139**, 7294-7301.